Temporal characteristic analysis of stepped pulse on hohlraum wall

Zhaoyang Jiao (焦兆阳)[1,2], Yanli Zhang (张艳丽)[1], Junyong Zhang (张军勇)[1], and Jianqiang Zhu (朱健强)[1*]

[1] *National Laboratory on High Power Laser and Physics, Shanghai Institute of Optics and Fine Mechanics, Chinese Academy of Sciences, Shanghai 201800, China*

[2] *University of Chinese Academy of Sciences, Beijing 100049, China*

[*] *Corresponding author: jqzhu@siom.ac.cn*

Received January 23, 2014; accepted March 5, 2014 posted online April 4, 2014

Temporal and spatial optical field distributions of a stepped pulse on the hohlraum wall are numerically analyzed using fast-Fourier-transform method combined with chromatographic theory. Changes in the rising edge of the stepped pulse caused by spatio-temporal effect are systematically studied. Results demonstrate that a certain time difference exists for the laser to reach the hohlraum wall because of oblique incidence, which causes distortion to the stepped pulse, especially to the rising edge. Influences of the incident angle, focal length, and width of the input rising edge on distortion degree of the stepped pulse are also discussed. This letter provides some guidance for targeting pulse shaping and synchronization.

OCIS codes: 260.1960, 250.5530, 320.5540.

doi: 10.3788/COL201412.042602.

In indirect, laser-driven inertial confinement fusion (ICF)[1−4], laser plasma interaction between a laser and a hohlraum wall produces X-ray that drives pellets to implode. The ICF target designs utilize three shockwaves to quasi-isentropically compress the capsule before the main compression wave drives the implosion of the fuel assembly[5,6]. The goal is to minimize the required drive energy by minimizing the entropy imparted to the capsule as it is implodes. Both the strength and timing of the shock and compression waves must be accurately set to achieve ignition[5]. The shocks must arrive at the inner DT-fuel surface in a tight sequence. The temporal profiles of the laser and resultant radiation temperature need to produce the desired shock strengths and timing. Thus, pulse shaping[7−9] is crucial to the shock timing[5,10,11]. The rising edge is an important part of pulse shaping. And the property of rising edge is also crucial to control hydrodynamic instability in the liquid-phase infiltration (LPI) process, which is proven in some way by the recent progress achieved by National Ignition Facility (NIF) in October 2013. Aiming to approach isentropic compression and improve implosion efficiency, a stepped pulse[6,12,13] is commonly employed in current physical experiments in targeting shaped pulses. In our previous work[14], however, a certain time difference existed for the laser to reach different positions on the hohlraum wall because of an oblique incidence. The beam propagation along the hohlraum wall is a push-broom process, and the evolution of the optical field on the hohlraum wall is a dynamic spatio-temporal process. This process is drastic on the rising edge of the pulse. We recently found that this effect can cause pulse distortion in the inputted stepped pulse on a scale of picoseconds (ps), which changes the steepness of the rising edge. The rising edge of the pulse is usually only about tens or hundreds of ps[6,15−17], although the pulse duration is in the nanosecond range. The stretched rising edge of the laser pulse would influence the shock-timing and then the isentropic compression. Meanwhile it may also weaken the collision effect of the shockwaves, which can cause failure of igniting the pellet. What's more, successful demonstration of laser fusion feasibility is critically dependent on the ability to drive the implosion with a very high degree of symmetry over the whole time of the target irradiation, achieved by a large number of synchronized incident laser beams symmetrically disposed around the target. If different laser beams of different incident angles undergo various pulse distortions, pulse synchronization of the multiple beams will be much more complicated than we thought. Thus, it is important and necessary to study the temporal characteristics of the stepped pulse on the hohlraum wall in order to accurately control the interaction between the laser and the hohlraum wall.

In this letter, temporal and spatial optical field distributions of a stepped pulse on a hohlraum wall are numerically analyzed with fast-Fourier-transform (FFT) method and chromatographic theory[13,17]. The effect of the spatio-temporal beam propagation on the stepped pulse is investigated in detail. Furthermore, the influences of the incident angle, focal length, and width of the input rising edge on the distortion degree are also concretely discussed.

According to the NIF's target chamber structure model, the parameters of the final target chamber structure are as follows[18]: laser wavelength of $\lambda = 0.351$ μm, beam size of 400 × 400 (mm), 10 order super-Gaussian beam with a waist radius of $\omega = 160$ mm. After a lens with focal length f=7700 mm is used, the laser beam passes through the orifice with diameter $2r$=3.5 mm into the cylindrical target chamber with diameter $2R = 15$ mm (Fig. 1(a)). In this scenario, the optical field distribution on the inclined cylindrical surface (θ=23.5°) is the main concern. According to the calculation model[14,18] based on chromatography theory, we need to calculate

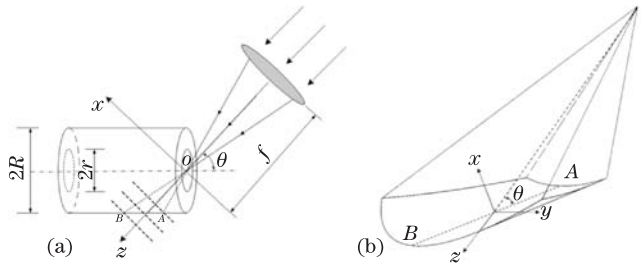

Fig. 1. (a) Diagram of ICF target chamber device and chromatography; (b) light spot pattern on the hohlraum wall.

multi-plane optical fields to fit the optical field on the cylindrical surface, as shown in Fig. 1(a). The z-direction represents the beam propagation direction (i.e., the focusing lens central axis). The x-direction is perpendicular to the z-direction in the paper plane, and the y-direction is perpendicular to the paper plane. The light spot pattern on the hohlraum wall is shown in Fig. 1(b).

When the angle between the optical axis and the cylindrical axis equals 23.5°, the distance between A and B along the optical axis is 2.25 mm and the corresponding time difference between A and B is approximately 7.64 ps. Because of the time difference, the evolution of the optical field on the hohlraum wall is a dynamic spatio-temporal process. The optical field changes with time and cannot get stabilized until the steady state is reached. When the front reaches position A, no light falls on position B, especially for a leading edge. When the light on position A reaches its maximum, the light on position B is still at the rising edge. Only when the light of both positions obtain their maximums on the flat top of the pulse will the optical field on the hohlraum wall become stable. Although the laser pulse experienced by each spatial point is the same, the rising edge of the input pulse is stretched from the perspective of the average effect of the optical field in the region between A and B on the hohlraum wall. In NIF pulse durations are in the nanosecond range, but the rising edge of the pulse is in the picoseconds range and the pulse distortions are also on the scale of a few ps. Recently NIF employed high foot pulse to achieve significant progress in the ICF research. Experiments show that the pulse edge is very important in the compression, whose property is crucial to control the LPI process. The stepped pulse employed in physical experiments usually has a very steep rising edge with a width of several ps. Given the spatio-temporal effect mentioned above, the stepped pulse undergoes severely distorted. The distortion can obviously change the property of the pulse edge. The following parameters are introduced to evaluate the deformation.

1) The average optical intensity $I_{\rm avg}$ on the hohlraum wall is given by

$$I_{\rm avg} = \sum_{i=1}^{N} I_i/N, \tag{1}$$

where i is the number of discrete samples along the x direction, i= 1, 2, 3$\cdots N$, and $I_i$is the optical intensity of the sample i. The intensity $I_{\rm avg}(t)$ could be utilized to describe the distorted pulse on the hohlraum wall and the new rising edge width after distortion can also be obtained.

2) The distortion degree M is defined as

$$M = (t_2 - t_1)/t_1, \tag{2}$$

where t_1 and t_2 represent the rising edge width of the input pulse and output pulses on the hohlraum, respectively. The distortion caused by the spatio-temporal effect can be effectively evaluated by the distortion degree M. The bigger M represents the more serious relative distortion.

Based on the calculation model, the evolution of the stepped pulse on the hohlraum wall is simulated and analyzed. Here a three-stepped pulse[12], commonly employed in physical experiments, is taken as the input. The width ratio of the three steps in the pulse is 1.5: 1: 0.5 (unit: ns) and the amplitude ratio is 1:4:16. The intensity distribution of the input pulse is shown in Fig. 2 and has two steep rising edges. For simplicity, the three-stepped pulse model is taken as piecewise functions and the rising edge is described by linear functions. The rising-edge widths of both the first and second steps are set at 10 ps.

Considering that the optical field distribution along the y direction is symmetrical[14], the optical field along the x direction is the main concern in this scenario.

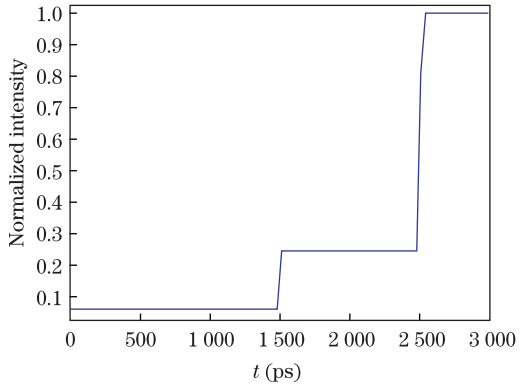

Fig. 2. Input three-stepped pulse.

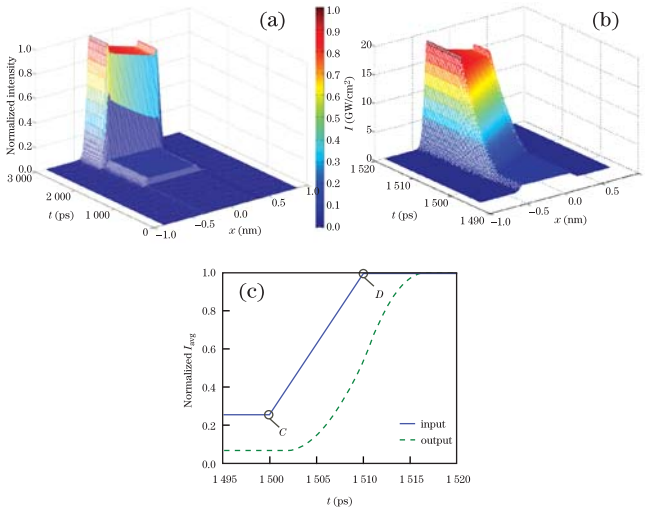

Fig. 3. (a) Normalized spatio-temporal optical intensity on the hohlraum wall; (b) output optical intensity for the first rising edge; (c) comparison of the input and output pulses.

Figure 3(a) shows the normalized spatio-temporal optical intensity on the hohlraum wall. The intensity distribution varies noticeably at the rising edge and finally tends to be steady at the flat top of the pulse. Therefore, only the rising edge of the laser pulse is significantly modified.

The first rising edge of the three-stepped pulse (i.e., from 1495 to 1520 ps) is extracted to analyze the temporal distortion of the stepped pulse caused by the spatio-temporal effect, especially in the rising edge. The corresponding optical intensity is shown in Fig. 3(b). The rising edge is obviously stretched, which means that pulse distortion occurs. Figure 3(c) shows a comparison between the normalized input pulse and the normalized average intensity ($I_{\rm avg}$) of the output pulse on the hohlraum wall. We can see that the rising edge width t_1 equals 10 ps and t_2 is approximately 17 ps. The corresponding distortion degree M is 0.7. For the input pulse, two inflection points, C and D, exist. After distortion, the properties of the two inflection points obviously change. The output pulse still begins to rising from point C, and rises gently at first and gradually becomes steeper. The rising edge of the output pulse is in a Gaussian-like shape, while that of the input pulse is in a steep linear type. For point D, an obvious delay for the output pulse is observed. The pulse distortion converts the steep turning at point D into a smooth entry to the flat top. In a word, after distortion, the pulse is stretched and also smoothened.

For further understanding of the distortion caused by the spatio-temporal effect, the influences of the incident angle, focal length, and rising edge width on the distortion degree of the stepped pulse are discussed, respectively.

Different incident angles exist for different beams, i.e., 23.5° and 30° for inner beams and 44.5° and 50° for outer beams. The above calculation is based on the incident angle of 23.5°. As shown in Fig. 4, the pulse is stretched by different degrees for different incident angles. When the incident angle θ becomes smaller, the width of the output rising edge is stretched to be larger. Accordingly, the smaller the θ, the larger the distortion degree of the pulse becomes (Fig. 5). This condition occurs because the smaller the θ, the more inclined the incident light and the longer the time difference on the hohlraum wall become. The corresponding spatio-temporal effect caused by the time difference is more serious. Thus, the distortion degree of the rising edge is also bigger. This difference should be noted when synchronizing the stepped pulse for multiple beams of different incident angles.

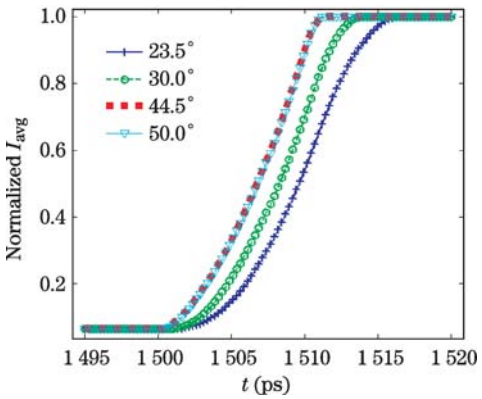

Fig. 4. Output pulse for different incident angles.

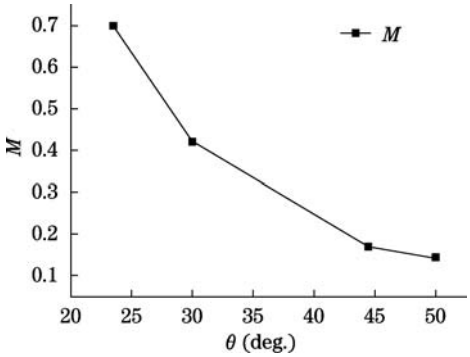

Fig. 5. Distortion degree for different incident angles.

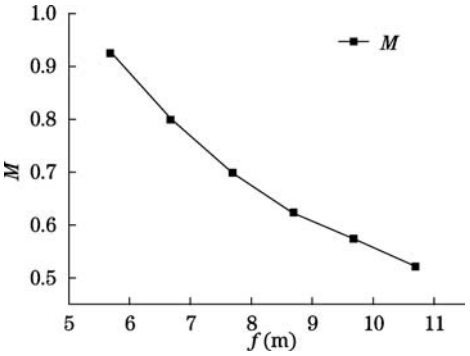

Fig. 6. Dependence of the distortion degree on the focal length.

F-number F_N is a critical parameter for the terminal optical system and given by

$$F_N = f/D, \tag{3}$$

where f is the focal length of the lens and D is the beam diameter. The variation of F-number will affect the light field of the system output. When the beam diameter is a constant, the F-number is proportional to the focal length. We set other parameters as default and change the focal length to ascertain what happens to the pulse shape. The relationship between the distortion degree and the focal length is shown in Fig. 6. As the focal length becomes shorter, the distortion degree of the pulse is bigger because when f is shorter, $F_{\rm N}$ is smaller and the beam divergence angle is larger. The time difference on the hohlraum wall is larger and the distortion degree of the laser pulse gets larger. Thus, we can increase the focal length to reduce this type of distortion effect.

The rising edge width used for all the above calculations is 10 ps to highlight the rising edge variation. In the experiments, however, stepped pulses with various rising edge widths are required. In this scenario, the influence of the rising edge width of the input pulse on the distortion degree is studied. As shown in Fig. 7, with increase in rising edge width, the distortion degree decreases. Since the distortion of the input pulse is mainly induced by the time difference of laser beam arriving on the hohlraum wall, when the time difference is a constant, the width of the rising edge of the output pulse t_2 is approximately equal to the sum of t_1 and the

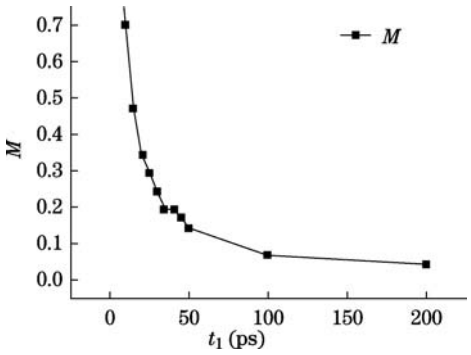

Fig. 7. Dependence of the distortion degree on the rising edge width.

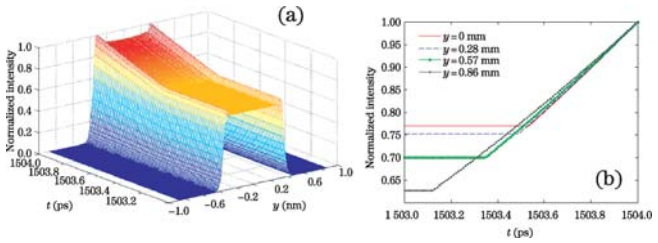

Fig. 8. (a) Normalized spatio-temporal intensity in the y direction; (b) pulse shape for different locations in the y direction.

time difference. According to Eq. (2), the distortion degree is inversely proportional to the input rising edge width t_1. That is to say, the steeper the input rising edge, the bigger the distortion degree becomes.

Meanwhile, it is found that there is a similar spatio-temporal effect in the y direction in the simulation. Here the optical field on the cross-section (x=0) is analyzed. Figure 8(a) shows the normalized spatio-temporal optical intensity in the y direction. The location (y=0) is the center of the light spot on the hohlraum wall. The rising edge of the spot center is about 3 ps later than the input pulse, which is caused by the previously mentioned spatio-temporal effects in the x direction. The pulse shapes of different locations are compared in Fig. 8(b). Some delays exist in the rising edge among different locations. The more to the middle, the more lag exists. This condition occurs because a cylindrical surface in the y direction is a curved surface, which is more concave in the middle. Thus the light reaches the middle locations later. This delay can also cause distortion to the pulse, thus stretching the rising edge. As can be seen from Fig. 8(b), the rising edge of the location (y=0) is about 0.4 ps later than that of the edge location (y=0.86 mm). The effect in the y direction is slightly different from that in the x direction. The delay in the y direction is symmetrical while the delay in the x direction is incremental. The overall delays in the x direction and y direction are 7.6 and 0.4 ps, respectively. Thus the corresponding spatio-temporal effect in the y direction is much weaker than in the x direction.

Like the x direction, the spatio-temporal effect in the y direction is also affected by the incident angle, the focal length, and the rising edge width. Similar analysis shows that when the incident angle becomes larger, the time delay between the middle and the edge becomes bigger and the corresponding pulse distortion is more serious. When the focal length increases, the overall delay decreases. So the pulse distortion becomes weaker. When the rising edge width becomes smaller, the relative pulse distortion is bigger.

For the second rising edge of the three-stepped pulse in Fig. 2, the law obtained above is also suitable. The temporal characteristics of the three-stepped pulse can thus be completely analyzed. In general, the stepped pulse distortion is mainly determined by the time difference on the hohlraum wall. The incident angle and focal length both have a big impact on the time difference and thereby on the pulse distortion. Nevertheless, the influence of the rising edge width is a type of sensitivity analysis that changes the relative distortion degree and not the absolute pulse distortion. The steeper the rising edge of the input pulse, the more serious the relative distortion degree becomes.

In conclusion, using FFT and chromatographic theory, the distortion of a stepped pulse on the hohlraum wall caused by the spatio-temporal effect is simulated and analyzed. Distortion mainly occurs on the rising edge of the laser pulse and the distortion degree is dependent on the incident angle, focal length, and input rising edge width. The incident angle and focal length directly affect the time difference and thereby the distortion while the influence of the rising edge width is a type of sensitivity analysis. The steeper the rising edge, the more serious the relative distortion becomes. When a stepped pulse with a very steep rising edge is needed, because of this kind of effect, the rising edge is stretched to decrease the steepness, which requires attention and vigilance. Without considering the pulse distortion effect, the pulse on the hohlraum wall would be different from the one designed by pulse shaping. Pulse distortions vary for different incident angles. Thus, pulse synchronization for the inner and outer beams needs involves different distortions. It will be much more difficult for the synchronization of multiple beams. What's more, as long as the laser beam is an oblique incident, the temporal distortion always exists. We could pre-compensate the pulse distortion by amending the objective function of pulse shaping, which will not be discussed in this paper due to space limitations. This study on temporal pulse shape distortion can provide some guidance for targeting pulse shaping and pulse synchronization, which also builds finer initial laser conditions to study the laser-plasma interaction in the hohlraum.

This work was supported by the National Natural Science Foundation of China (Nos. 11104296 and 61205212) and the Chinese and Israeli Cooperation Project on High Power Laser Technology (No. 2010DFB70490).

References

1. K. A. Brueckner and S. Jorna, Rev. Mod. Phy. **46,** 325 (1974).
2. J. Lindl, Phys. Plasmas **2,** 3933 (1995).
3. J. D. Lindl, *Inertial confinement fusion*: *the quest for ignition and energy gain using indirect drive* (Springer, 1998). Vol. 2998.
4. F. Liu, Z. Liu, L. Zheng, H. Huang, and J. Zhu, High Power Laser Sci, Eng. **1,** 29 (2013).
5. T. Boehly, D. Munro, P. Celliers, R. Olson, D. Hicks, V.

Goncharov, G. Collins, H. Robey, S. Hu, and J. Morozas, Phys. Plasmas **16,** 056302 (2009).

6. S. W. Haan, S. M. Pollaine, J. D. Lindl, L. J. Suter, R. L. Berger, L. V. Powers, W. E. Alley, P. A. Amendt, J. A. Futterman, and W. K. Levedahl, Phys. Plasmas **2,** 2480 (1995).
7. D. Huang, W. Fan, X. Li, and Z. Lin, Chin. Opt. Lett. **10,** 21406 (2012).
8. Z. Liu, P. Li, J. Chi, and X. Zhang, Chin. Opt. Lett. **10,** 11404 (2012).
9. C. Xu, L. Jiang, N. Leng, Y. Yuan, P. Liu, C. Wang, and Y. Lu, Chin. Opt. Lett. **11,** 41403 (2013).
10. V. Goncharov, O. Gotchev, E. Vianello, T. Boehly, J. Knauer, P. McKenty, P. Radha, S. Regan, T. Sangster, and S. Skupsky, Phys. Plasmas **13,** 012702 (2006).
11. D. H. Munro, P. M. Celliers, G. W. Collins, D. M. Gold, L. B. Da Silva, S. W. Haan, R. C. Cauble, B. A. Hammel, and W. W. Hsing, Phys. Plasmas **8,** 2245 (2001).
12. S. W. Haan, T. Dittrich, M. Marinak, and D. Hinkel, *Design of Ignition Targets for the National Ignition Facility* (Elsevier, 1999).
13. W. Wang, R. Zhao, J. Su, H. Li, Y. Liang, L. Mo, F. Wang, L. Liu, Z. Sun, and Q. Zhu, Acta Opt. Sin. (in Chinese) **30,** 1051 (2010).
14. Z. Jiao, Y. Zhang, J. Zhang, and J. Zhu, High Power Laser Sci. Eng. **1,** 88 (2013).
15. B. Canaud and M. Temporal, New J. Phys. **12,** 043037 (2010).
16. J. Knauer, K. Anderson, R. Betti, T. Collins, V. Goncharov, P. McKenty, D. Meyerhofer, P. Radha, S. Regan, and T. Sangster, Phys. Plasmas **12,** 056306 (2005).
17. R. Olson, J. Porter, G. Chandler, D. Fehl, D. Jobe, R. Leeper, M. Matzen, J. McGurn, D. Noack, and L. Ruggles, Phys. Plasmas **4,** 1818 (1997).
18. D. Huang, X. Yao, X. Zhao, C. Zhang, C. Wu, and F. Gao, High Power Laser Particle Beams (in Chinese) **24,** 69 (2012).